



## Structure of molten Al and eutectic Al–Si alloy studied by neutron diffraction

U. Dahlborg<sup>a</sup>, M.J. Kramer<sup>b</sup>, M. Besser<sup>b</sup>, J.R. Morris<sup>c</sup>, M. Calvo-Dahlborg<sup>a,\*</sup>

<sup>a</sup> GPM, UMR6634, University of Rouen, BP12, 76801 Saint-Etienne du Rouvray Cedex, France

<sup>b</sup> Ames Laboratory, Iowa State University, Ames, IA 50014, USA

<sup>c</sup> Oak Ridge National Laboratory, P. O. Box 2008, Oak Ridge, TN 37831-6115, USA

### ARTICLE INFO

#### Article history:

Received 24 August 2012

Received in revised form 20 September 2012

Available online 24 November 2012

#### JEL classification:

61.25.Mv

61.05.fm

#### Keywords:

Structure;

Al–Si;

Neutron diffraction;

Melt;

Superheat

### ABSTRACT

The structure of molten eutectic  $\text{Al}_{87.8}\text{Si}_{12.2}$  alloy has been studied by neutron diffraction during a temperature cycle. For comparison measurements were performed on pure molten Al. The measurements show that the alloy after heating above the liquidus contains particles of two kinds, aluminum-rich and silicon-rich. The silicon-rich particles are partly dissolved after a further heating. Earlier published data obtained by the  $\gamma$ -ray absorption technique of the density of the molten eutectic Al–Si alloy had demonstrated the existence of two temperatures above the liquidus temperature: A dissolution temperature  $T_d$ , at which the microstructure of the melt inherited from the ingot starts to dissolve and a branching temperature,  $T_b$ , at which the melt reaches a fully mixed state. The highest temperature that was possible to reach during the neutron experiments lies between  $T_d$  and  $T_b$ . The obtained results support these conclusions that molten alloys after melting are inhomogeneous up to a temperature well above the liquidus. Moreover, the difference in shape between the static structure factors measured by neutron and X-ray diffraction on molten aluminum is observed and is found to be more accentuated and to extend to larger wavevectors than in earlier works.

© 2012 Elsevier B.V. All rights reserved.

### 1. Introduction

The conditions in which melt solidification occurs greatly influence the structure, microstructure and properties of the resulting sample. To achieve the control of the properties of specimen through the understanding of the influence of the various synthesis conditions has been the aim of numerous studies in all fields of materials research. In particular, the effect of superheating the melt before quench has been investigated on different types of materials such as metallic glass ribbons and bulks [1–10], Al-based alloys [11–13], Ti–Al alloys [14], magnesium alloys [15], Sn–Pb alloys [16], Ni-based superalloys [17,18], nanocomposites [19]. Different solidification rates have also been tried [20–24] as well as different mixing procedures [25–28]. However, the conclusions from these studies have mostly been drawn from investigation of the morphology, structure and properties of the solidified state, rarely from the precursor liquid phase itself. Thus the interpretations of the liquid state have often been indirect.

With specific regard to Al–Si alloys, there exist a large bibliography on reported effect of superheat on the properties of the solidification product for standard alloys such as A356 [29,30] or A390 as well as binary alloys [31–34]. The reported effects are generally a finer and/or more uniform microstructure as well as an increase of yield strength, tensile strength and ductility in the samples produced with superheat

of the melt before solidification [35–37]. The structure for different compositions, including liquid Al [38–47] and at different temperatures as well as the effect of the addition of small amounts of a third element have been extensively investigated on an atomic scale by neutron and X-ray diffraction techniques or microscopy [48–55 and references therein,56–58].

However, from all these studies it is not possible to obtain a clear description of the structure as well as of the physical properties because the presented results differ substantially. Even a fundamental quantity in a diffraction experiment such as the height of the main peak of the static structure factor differs significantly between different published results as can be seen in Table 1 in which some selected results are listed. In this connection it should be emphasized that, as was first stressed in [59], static structure factors measured by neutron and by X-ray techniques are not expected to be identical because of the different scattering mechanisms in the two cases. This fact is experimentally verified by the values in Table 1.

The disparity between published results is also true for another fundamental quantity as the density. Thus, in three recent performed investigations of this quantity utilizing different experimental techniques (attenuation of  $\gamma$ -rays [60], the sessile drop method [61], and the Archimedian method [62]), the quoted densities for molten eutectic Al–Si alloy at 973 K differ by about  $\pm 1\%$ . In view of the achievable accuracy of the three techniques this may not be surprising but for an adequate comparison to calculated physical properties it might not be good enough. However, the discrepancy between the different results

\* Corresponding author. Tel.: +33 232955336.

E-mail address: [monique.calvo-dahlborg@univ-rouen.fr](mailto:monique.calvo-dahlborg@univ-rouen.fr) (M. Calvo-Dahlborg).

**Table 1**

Position and height of the main peak of the structure factor  $S(Q)$  for molten Al as reported in various publications. ND denotes neutron diffraction and XD X-ray diffraction.

Reference	Technique	Temperature (K)	Position of main peak ( $\text{\AA}^{-1}$ )	Height of main peak
Iqbal et al. [38]	ND	936	2.68	2.44
Mudry et al. [39]	XD	938	2.70	2.47
Takeda et al. [40,41]	ND	943	2.68	2.43
Waseda [42]	XD	943	2.71	2.48
Larsson et al. [43]	ND	950	2.70	2.20
Gabathuler et al. [44]	ND	953	2.70	2.25
Becker et al. [45]	XD	973	2.67	2.36
Roik et al. [46]	XD	973	2.68	2.12
Present work	ND	973	2.68	2.26
Stallard et al. [47]	ND	976	2.67	2.17
Jovic et al. [56]	ND	980	2.69	2.21

of measurements of the same physical properties and also their anomalous temperature dependences can in many cases be interpreted in terms of the structural inhomogeneities present after melting in the molten alloy and their dissolution when the liquid is heated further [50,63–65 and references therein]. The dissolution starts at a temperature  $T_d$  and at a branching temperature  $T_b$  well above the liquidus all inhomogeneities are dissolved. Some physical properties are thus different in heating and cooling modes. This is exemplified in Fig. 1 where density measurements taken from [11,60] for the eutectic molten Al–Si alloy during heating and cooling are presented. The difference between the heating and cooling data in the solid state ( $T < 850$  K) is due to the fact that the ingot did not completely fill the BeO container and also to the slow disappearance of the oxide layer with increasing temperature. The existence of a branching temperature at about 1560 K is clearly seen in Fig. 1 and indicated by the arrow. The phase diagram for the Al–Si system is a simple eutectic. In the solid phase the solubility of Si in Al is low, about 1.6 at%, while a considerable increase in solubility has been observed under high pressure [66] and by rapid quenching [20]. The results in Fig. 1 suggest that there exist thermodynamically stable phases in the molten state and that the relative amount of these phases also vary with alloy composition [63,65,67,68]. Similar anomalous behaviors have been observed in viscosity [69–72], resistivity [72–74], ultrasound velocity [70] and internal friction [21] measurements for many molten alloys.

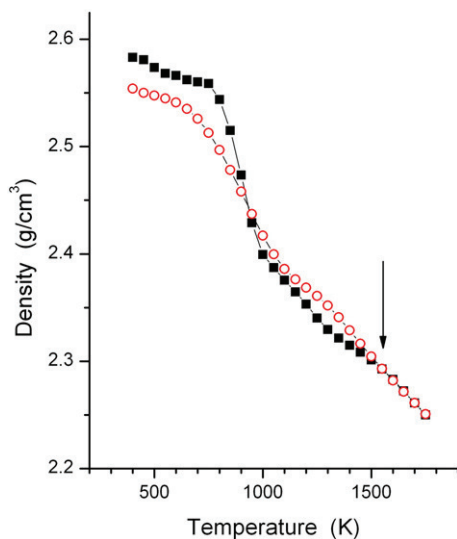


**Fig. 1.** The density of the eutectic  $\text{Al}_{87.8}\text{Si}_{12.2}$  alloy measured during heating (full squares) and subsequent cooling (empty circles). The arrow indicates the estimated branching temperature  $T_b$ .

However, the value of both the dissolution and branching temperatures is not sharp and it depends sensitively on the presence of very small amounts of impurities [11,63]. A strong support on atomic level for this picture has been obtained from small angle neutron scattering measurements [64,65]. *Ab initio* molecular dynamics simulations have also been carried out on the Al–Si system [75–77]. The number of atoms in some simulations is small (about 50 to 200) and for dilute systems they suffer significantly from bad statistics [78]. However, recent increases in computational efficiency simulations have enabled to include 500 atoms in a study of the eutectic Al–Si alloy [77]. Nevertheless, the comparison to accurate experimental data is essential for their validation. The alloy compositions as well as the alloy temperatures are not always the same in simulations and experiments and detailed comparisons are accordingly often difficult to make. Another complicating factor in such comparisons is the considerable difference between experimentally determined static structure factors.

One of the aims of the present work is to add to the clarification of the reason for the above-mentioned variation of the physical properties. Thus, experimental results on the structure on an atomic scale of the molten eutectic Al–Si alloy obtained by the neutron diffraction technique, obtained during heating and cooling are presented and discussed. In order to demonstrate the accuracy needed to obtain the desired information the adopted data correction procedure is discussed in detail. A preliminary interpretation of some of the data presented below has been earlier briefly published [79] and the microstructure, i.e. the structure on a length scale larger than about 1 nm, is discussed in another paper [65].

## 2. Theoretical background

The measured intensity in a diffraction experiment on a disordered material is proportional to the total static structure factor  $S(Q)$  that for a binary system in the Faber–Ziman formalism is given by

$$S(Q) = \frac{\left\{ I_a^{\text{coh}}(Q) - \left[ \langle b^2 \rangle - \langle b \rangle^2 \right]^2 \right\}}{\langle b \rangle^2} = \sum_{\alpha} \sum_{\beta} c_{\alpha} c_{\beta} b_{\alpha} b_{\beta} S_{\alpha\beta}(Q) / \langle b \rangle^2 \quad (1)$$

$I_a^{\text{coh}}(Q)$  is the intensity per atom of coherently scattered neutrons and  $c_i$  and  $b_i$  are the concentration and scattering amplitude of atoms  $\alpha$  and  $\beta$ , respectively.  $\langle b \rangle$  is equal to  $c_{\alpha} b_{\alpha} + c_{\beta} b_{\beta}$  and  $\langle b^2 \rangle$  to  $c_{\alpha} b_{\alpha}^2 + c_{\beta} b_{\beta}^2$ .  $S_{\alpha\beta}(Q)$  is the partial structure factors.  $Q$  is the neutron wavevector transfer in the scattering process and it is given by  $Q = 2k \sin(2\theta)$  where  $k$  is the neutron wavevector and  $2\theta$  is the scattering angle. From the definition it follows that  $S(Q)$  is equal to one at large  $Q$ . The scattering amplitudes for Al and Si are 3.45 and 4.15 fm and thus the relative weight factors in Eq. (1) for the homogeneous eutectic Al–Si alloy are 0.64, 0.32 and 0.04, for  $S_{\text{AlAl}}(Q)$ ,  $S_{\text{AlSi}}(Q)$  and  $S_{\text{SiSi}}(Q)$ , respectively.

The static structure factor  $S(Q)$  is defined as the zero energy moment of the dynamic scattering function  $S(Q, E)$ . Accordingly,  $S(Q)$  is defined for a specific  $Q$  value as

$$S(Q) = \int_{\frac{Q}{\infty} = \text{const.}}^{+\infty} S(Q, E) dE \quad (2)$$

## 3. Experimental details

The neutron diffraction experiments were performed on the D4C diffractometer at the Institute Laue-Langevin, Grenoble, France [80]. The wavelength of the incident neutrons was 0.703  $\text{\AA}$  and accordingly the corresponding  $Q$  range was  $0.4 < Q < 16.5 \text{\AA}^{-1}$ . The Al–Si sample

was of eutectic composition, Al<sub>87.8</sub>Si<sub>12.2</sub>, and measured in a temperature cycle, at 973 K, at 1373 K and again at 973 K. The liquidus temperature of this alloy is 850 K. For reference purposes a sample of pure Al was measured at two temperatures, 973 K and 1373 K [\*]. The measurement time was three hours and the samples were kept about ten minutes at the desired temperature before recording started. The maximum temperature possible to reach with the available furnace was thus about 200 K lower than the branching temperature, 1560 K, shown in Fig. 1. The dissolution temperature,  $T_d$ , is estimated for this alloy to 1350 K ± 30 [11,69].

The sample ingots were made from 99.999% pure starting materials. The alloys were arc-melted into buttons and then drop cast into 9.5 mm diameter copper moulds. As Al-based molten alloys are extremely corrosive the samples were contained in very thin-walled cylindrical alumina containers of diameter slightly less than 10 mm and wall thickness of about 50 microns. The alumina cans were in turn inserted in vanadium containers. Even if the amount of alumina present in the neutron beam was very small, small Bragg peaks were visible in the measured diffraction patterns. However, these could to a satisfactory extent be accounted for during the data treatment. Nevertheless, in some cases some uncertainties remain in the corrected data due to different preferential orientations of the alumina grains in the measurements on the molten samples and on the empty containers. The cubic to monoclinic phase transformation that takes place in the alumina system at high temperatures has also complicated the data correction procedure, though to a small extent (see text below).

**4. Data treatment**

The measured data were corrected for container scattering, absorption and geometrical effects using standard straightforward procedures. Adequate corrections for multiple and inelastic scattering is of great importance for the accuracy of a determined  $S(Q)$  but are considerably more difficult to obtain. In this work the multiple scattering was obtained by iterative calculations with the MSCAT computer code [81] and the correction for inelastic scattering was considered in great detail according to the scheme described below.

In a diffraction experiment at a continuous neutron source the number of scattered neutrons is measured as a function of the scattering angle  $2\theta$  and not at constant  $Q$ . Contrary to the definition of  $S(Q)$  in Eq. (2), the measured static structure factor  $S(Q_0)_{meas}$  is thus in this case given by

$$S(Q_0)_{meas} = \frac{1}{\varepsilon(k_0)} \int_{-\infty}^{E_0} \frac{k}{k_0} S(Q, E) \varepsilon(k) dE \quad (3)$$

$2\theta = \text{const.}$

$Q_0$  is the wavevector transfer for elastically scattered neutrons and  $k_0$  and  $k$  are the wavevectors of the incident and scattered neutron, respectively.  $E_0$  is the energy of the incident neutron. The wavevector dependent detector efficiency which is an instrument parameter is given by  $\varepsilon(k)$ . The procedure to correct a measured diffraction pattern and arrive to an exact  $S(Q)$  is usually called the Placzek (or the inelasticity) correction. It may be anticipated from Eq. (3) that the larger the energy range of  $S(Q, E)$ , the larger the difference between  $S(Q_0)_{meas}$  and the real  $S(Q)$ . The difference is more accentuated for alloys consisting of heavy atoms than for light ones. Several more or less approximate recipes exist which have been developed in order to accurately correct a neutron diffraction experiment for the inelasticity effect [82–84]. A relation between  $S(Q_0)_{meas}$  and the real  $S(Q)$  may conveniently be defined as

$$P(Q) = \frac{S(Q_0)_{meas}}{S(Q)} - 1 \quad (4)$$

In order to obtain an accurate  $P(Q)$  it is thus necessary to know  $S(Q, E)$  for the scattering system. This is seldom the case and several approximations of  $P(Q)$  based on series expansions of  $S(Q, E)$  are used. However, these approximations are not accurate enough to yield a corrected  $S(Q)$  with a sufficient accuracy to make conclusive a detailed comparison to theoretical models and different kinds of molecular dynamics simulations.

For liquid aluminum the situation is different as  $S(Q, E)$  could be determined from both inelastic neutron and X-ray scattering experiments [85,86].  $P(Q)$  was calculated assuming that the simple viscoelastic model (VEL) [87,88] is accurate enough for our purpose, with parameters chosen in accordance with experimental results and an included recoil term. It might be argued that the use of the VEL is not a good representation of  $S(Q, E)$  for small  $Q$  but it has the merit that for larger  $Q$  it approaches correctly the gas model. However, the essential factor to achieve an appropriate calculation of  $P(Q)$  is to use an expression of  $S(Q, E)$  which describes as closely as possible the  $Q$  dependence while the influence of the  $E$  variation is of minor importance. In order to test the applicability of the VEL model calculations were performed with different parameter sets. The variation in the calculated  $P(Q)$ s was found to be negligible in comparison to the magnitude of  $P(Q)$ .

There exists to the knowledge of the authors no determination of the dynamic scattering function  $S(Q, E)$  for molten Al–Si. However, as the  $Q$  dependence of  $S(Q)$  for molten Al and molten Al–Si alloys are very similar, the difference in shape of the  $S(Q, E)$ s for the two systems is not expected to be significant when calculating an adequate  $P(Q)$  for an Al-rich alloy. This assumption is supported by calculations using the above approach applied to molten Al–Cu alloys for which  $S(Q, E)$  has been determined by neutron inelastic scattering [55]. It should be mentioned that because the Al–Si alloy consists of light elements an exact correction for the inelasticity effect as outlined above has to be made in order to arrive at an accurate  $S(Q)$  from a neutron diffraction measurement.

Some commonly used approximations in order to correct a measured  $S(Q)$  for the inelasticity effects are compared in Fig. 2. The most notable feature is the oscillatory nature of the  $P(Q)$  calculated

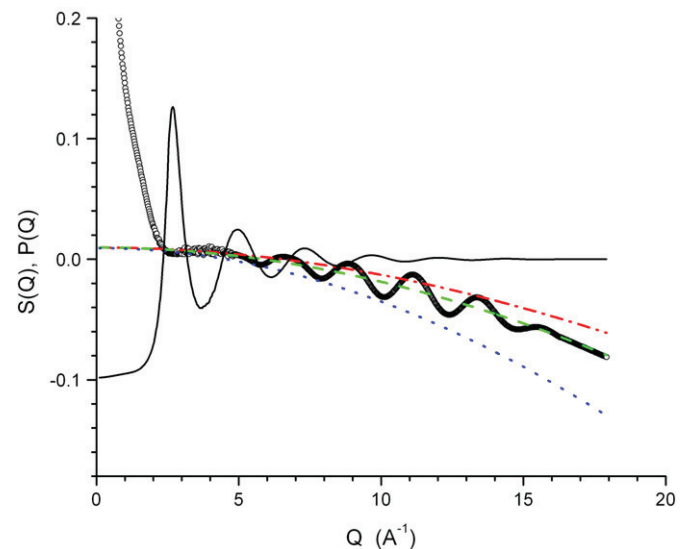


**Fig. 2.** The calculated quantity  $P(Q) = (S(Q)_{meas}/S(Q)) - 1$  for molten Al calculated with the following assumptions; i) assuming that the scattering system is an ideal gas (red dash-dotted line), ii) assuming that the scattering system is an ideal gas but including neutron recoil (green dashed line), iii) according to the moment expansion of  $S(Q, E)$  [82] (blue dotted line) and iv) assuming the scattering kernel being described by the viscoelastic model, including the recoil term, with parameters relevant for liquid Al [85–88] (black circles). For comparison the shape of the fully corrected  $S(Q)$  is indicated (black full line)

from the viscoelastic model. Although the amplitude of the oscillations is rather small they are remarkably not in phase with the oscillations in  $S(Q)$ . This fact has a clear influence on the position and amplitude of peaks in the pair distribution function  $g(R)$  determined by Fourier transformation of  $S(Q)$ . However, the oscillatory behavior of  $P(Q)$  is expected as  $S(Q, E)$  cannot be considered as a monotonous function for coherently scattering liquid metals and alloys and as the static approximation ( $|\mathbf{k}| = |\mathbf{k}_0|$ ) cannot be used. Furthermore, it is at once seen in Fig. 2 that, as already emphasized in [83], neither the ideal gas model, with or without a recoil term, nor the moment expansion is accurate enough to use in order to correct neutron diffraction measurements. It has been suggested that a replacement of the atomic mass  $M$  by an effective mass  $M_{\text{eff}} = M/S(Q)$  would make the use of these simple models possible [83]. However, calculations show that this does not correctly reproduce the oscillations in the  $P(Q)$  calculated from the viscoelastic model. It is also worth noticing in Fig. 2 that for  $Q$  less than about  $1.5 \text{ \AA}^{-1}$   $P(Q)$  is rapidly increasing with decreasing  $Q$ . This increase is due to the interference between the sound velocity in the scattering system and the velocity of the incident neutron.

## 5. Results and discussion

The fully corrected static structure factors  $S(Q)$  at 973 K and at 1373 K [\*] for liquid Al are shown in Fig. 3(a). The only significant difference between the two  $S(Q)$ s is as expected a general smearing out of the oscillations and a slight change of all features to smaller  $Q$  at the highest temperature. For example, the height of the main peak for Al at 973 K is in the present work found to be 2.26 while at 1373 K it has decreased to 1.95. Taking into account the temperature differences the value at 973 K (2.26) compares, as can be seen in Table 1, well with earlier neutron diffraction results. The difference between the  $S(Q)$ s in Fig. 3(a), shown in Fig. 3(b), indicates a smooth change in melt structure between 973 K and 1373 K. The small feature of a magnitude less than 0.005 seen at about  $3.8 \text{ \AA}^{-1}$  is, as was indicated above, due to an inaccuracy in the correction for the  $\text{Al}_2\text{O}_3$  container scattering.

The fully corrected static structure factors  $S(Q)$  at 973 K and at 1373 K for the eutectic molten Al–Si alloy are shown in Fig. 4(a) and the difference between the two in Fig. 4(b). As was the case for liquid Al there is a general smearing out although of smaller magnitude of the oscillations with increasing temperature. Thus the height has decreased from 2.05 to 1.84 when the temperature increased from 973 K to 1373 K. Literature measurements show a large spread in the height of the main peak (see Table 2). However, as is seen in Fig. 4(b), the difference curve is not as smooth as was the case for pure Al which indicates that the change in structure occurring between the two temperatures is considerably larger in the alloy. One can especially note that the difference in the amplitude of the main peak is smaller for the alloy but that the difference stretches over a wider  $Q$  range. Moreover, the difference data show more irregularities as compared to liquid Al (Fig. 3(b)). It should though be noted that the small bump at about  $3.8 \text{ \AA}^{-1}$  identified above as an artifact in Fig. 3(b) is also present in Fig. 4(b). Thus, in order to check whether the observed irregularities in Fig. 4(b) are due to a presence of Si particles the diffraction peaks positions in diamond structure Si are shown as vertical bars. Correspondence can be found for the (111) and the (220) peaks at about  $2.0$  and  $3.3 \text{ \AA}^{-1}$ , respectively, but not for higher order reflections. It is worth to note that for amorphous Si two first sharp peaks have been observed at about  $2.0$  and  $3.5 \text{ \AA}^{-1}$  [90]. Furthermore in supercooled liquid Si the position of the main peak is at about  $Q = 2.7 \text{ \AA}^{-1}$  and it has a pronounced shoulder at about  $3.6 \text{ \AA}^{-1}$  [91]. The shoulder resembles the shape of the difference data between 3 and  $3.5 \text{ \AA}^{-1}$ . Accordingly, the above observations allow to conclude that the Al–Si eutectic alloy after melting up to

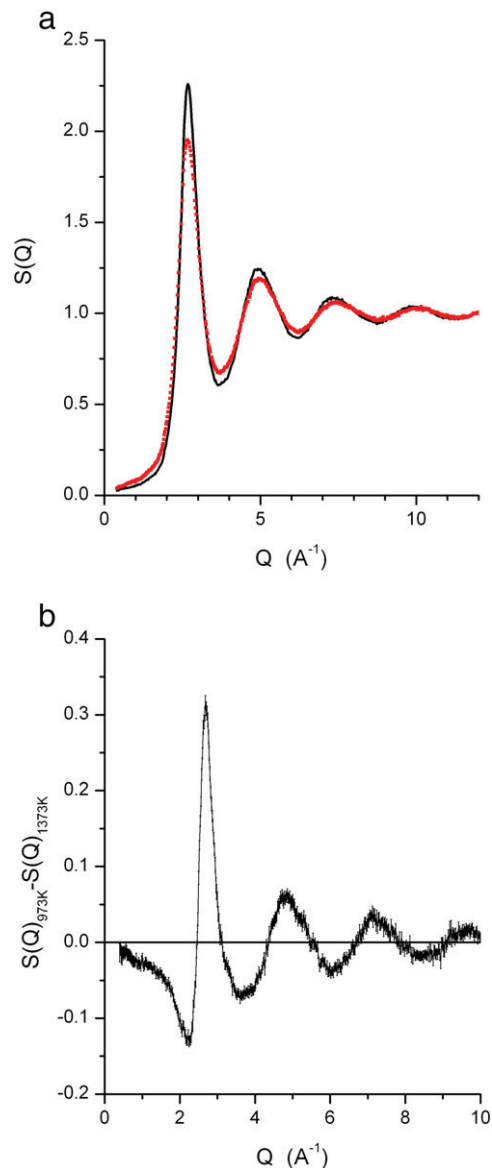
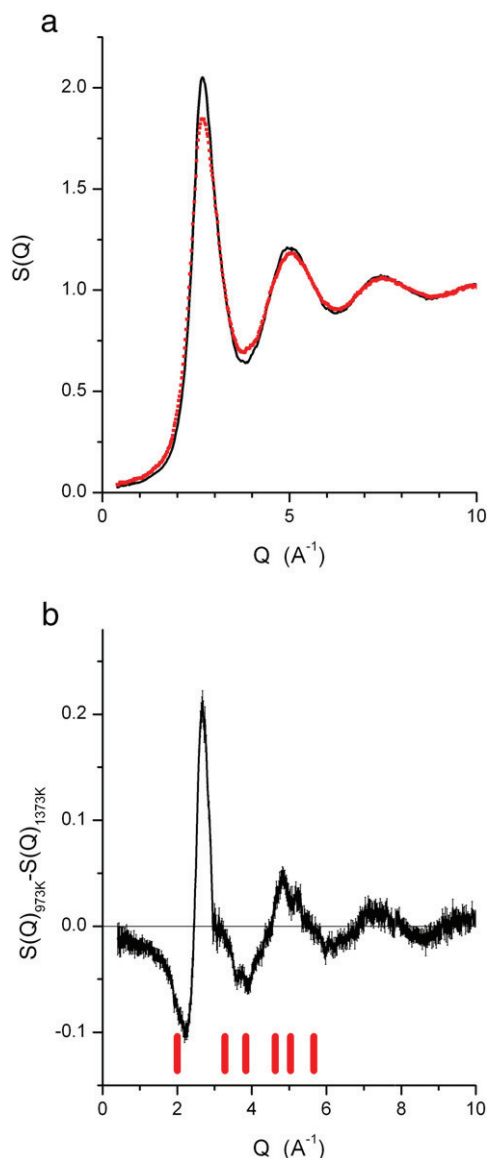


Fig. 3. (a) Fully corrected static structure factors  $S(Q)$  for liquid Al at 973 K (black dots) and 1373 K (red empty circles). (b) The difference,  $S(Q)_{973\text{K}} - S(Q)_{1373\text{K}}$ , between the two  $S(Q)$ s shown in (a).

1373 K can be considered as a two-phase system, one aluminum-rich and one silicon-rich part.

Wang et al. observed in X-ray diffraction measurements a prepeak in  $S(Q)$  around  $Q = 1.2 \text{ \AA}^{-1}$  when heating an Al–14 wt% Si to 1123 K [61]. The existence of this prepeak was interpreted to be a sign of Si atom clustering and it was correlated with a measured volume expansion of the hypereutectic melt during heating. However, no prepeak is seen either in the patterns displayed in Fig. 4(a) or for the  $\text{Al}_{88}\text{Si}_{12}$  alloy presented in [54]. Furthermore, the melting temperature to which the alloy is melted in [61] is well below the estimated dissolution temperature,  $T_d$ , for this alloy,  $1350 \text{ K} \pm 30$  [11,69]. It should also be mentioned that the authors in [50] did not report on the existence of a prepeak in the pure alloy but only after an addition of 0.2% Sb. A similar effect was observed in [54] after the addition of 5at% Ni to the  $\text{Al}_{88}\text{Si}_{12}$  alloy. It might thus be conjectured that the prepeak observed and discussed in [61] originates from a surface contamination of the sample or from a clustering of the impurity atoms. This conclusion is supported by recent large-scale ab initio molecular dynamics simulations [77]. Furthermore, significant effects of small amounts of



**Fig. 4.** (a) Fully corrected static structure factors  $S(Q)$  for molten  $\text{Al}_{87.8}\text{Si}_{12.2}$  at 973 K (black dots) and 1373 K (red empty circles). (b) The difference,  $S(Q)_{973\text{K}} - S(Q)_{1373\text{K}}$ , between the two  $S(Q)$ s shown in (a). The vertical bars at the bottom of the picture indicate the diffraction peak positions in diamond structure Si.

**Table 2**

Position and height of the main peak of the structure factor  $S(Q)$  for molten Al–Si alloys of near-eutectic composition as reported in various publications. ND denotes neutron diffraction and XD X-ray diffraction, respectively.

Reference	Technique	Alloy	Temperature (°K)	Position of main peak ( $\text{\AA}^{-1}$ )	Height of main peak
Gabathuler et al. [44]	ND	$\text{Al}_{89}\text{Si}_{11}$	858	2.72	2.23
Srirangam et al. [54]	XD	$\text{Al}_{88}\text{Si}_{12}$	867	2.68	2.18
Bian et al. [50]	XD	$\text{Al}_{87}\text{Si}_{13}$	893	2.68	2.56
Bian, Wang [89]	XD	$\text{Al}_{87}\text{Si}_{13}$	948	not given	1.87
Shtablavyi et al. [58]	XD	$\text{Al}_{88}\text{Si}_{12}$	950	2.66	1.95
Srirangam et al. [54]	XD	$\text{Al}_{88}\text{Si}_{12}$	973	2.68	2.06
Present work in heating mode	ND	$\text{Al}_{87.8}\text{Si}_{12.2}$	973	2.67	2.05
Present work in cooling mode	ND	$\text{Al}_{87.8}\text{Si}_{12.2}$	973	2.68	2.12

impurities on the structure and the physical properties of molten Al–R (R = rare earth elements) alloys has been shown in [72].

As was mentioned in the introduction and exemplified in Fig. 1 in case of eutectic Al–Si several physical properties of molten alloys depend on the thermal history of the melt. In order to investigate whether superheating has any effect on the structure as revealed in  $S(Q)$  of the molten alloy neutron diffraction measurements were performed at 973 K on heating and at the same temperature after that the melt had been heated to 1373 K during three hours. The difference between the two  $S(Q)$ s,  $S(Q)_{\text{Heating}} - S(Q)_{\text{Cooling}}$ , is shown in Fig. 5. A pronounced difference is clearly seen over the whole  $Q$  range. Especially, the main peak of  $S(Q)$  has become considerably sharper by the overheating of the melt (see Table 1) while its position has changed slightly to a larger  $Q$ . As the two measurements were performed at the same temperature it can be concluded that the melt has become more homogeneous.

As mentioned in the introduction the scattering mechanisms for neutron and X-ray scattering are different. Neutrons are scattered by the nuclei while X-rays are scattered by electrons, including both the electrons bound to the ions and the valence electrons. Thus the detailed shapes of  $S(Q)$  determined by the two scattering methods are different and it has been shown that it is possible to use this difference in order to determine the electron–ion correlations in a liquid metal [40,41,59,92]. The neutron measured  $S_N(Q)$  for molten Al at 973 K presented above (Fig. 3(a)) is in Fig. 6(a) compared to the  $S_X(Q)$  measured by synchrotron X-rays from [93]. The difference, in Fig. 6(b) presented as  $D(Q) = Q[S_X(Q) - S_N(Q)]$ , seems to be of considerably larger amplitude, to have more significant periodicity and to extend to larger  $Q$  values than the same quantity published in [40,41]. The difference in the phase of the oscillations of  $S_N(Q)$  and  $S_X(Q)$  furthermore accentuates the importance of an accurate correction for inelastic scattering as demonstrated in Fig. 2. The oscillations of  $D(Q)$  for molten eutectic Al–Si as obtained by combining data from the present work and [54] is of very much smaller amplitude that suggests that the number of valence electrons is small in the molten alloy. This will be further explored in a subsequent report.

For the sake of completeness the pair distribution functions  $g(R)$  obtained by direct Fourier transformation of the measured  $S(Q)$ s for liquid Al and eutectic Al–Si at 973 and 1373 K are shown in Fig. 7, (a) and (b), respectively. The oscillations for small  $R$  are small giving confidence to the accuracy of the data correction procedure presented above. Coordination numbers  $N$  have been calculated by choosing the position  $R_{\text{min}}$  of first minimum of  $g(R)$  as cut-off distance.  $N$  was for Al found to be slightly larger than 12 at both 973 K and 1373 K and for

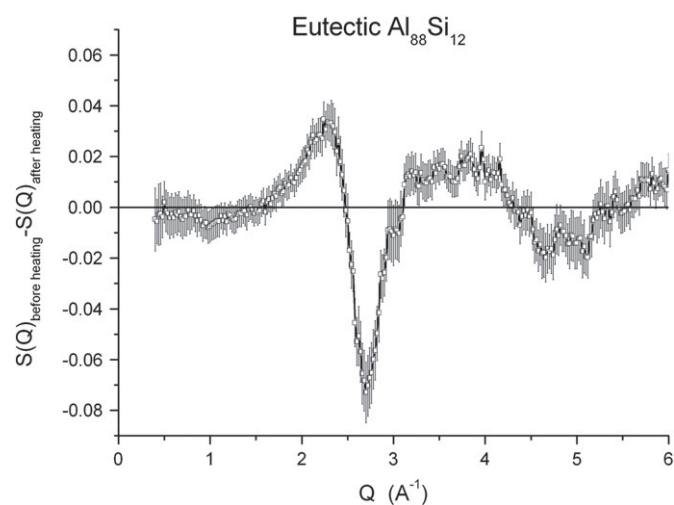


**Fig. 5.** The difference,  $S(Q)_{\text{Heating}} - S(Q)_{\text{Cooling}}$ , between  $S(Q)$  measured for molten  $\text{Al}_{87.8}\text{Si}_{12.2}$  in heating mode at 973 K and  $S(Q)$  measured at the same temperature but after that the molten alloy has been kept at 1373 K during three hours.

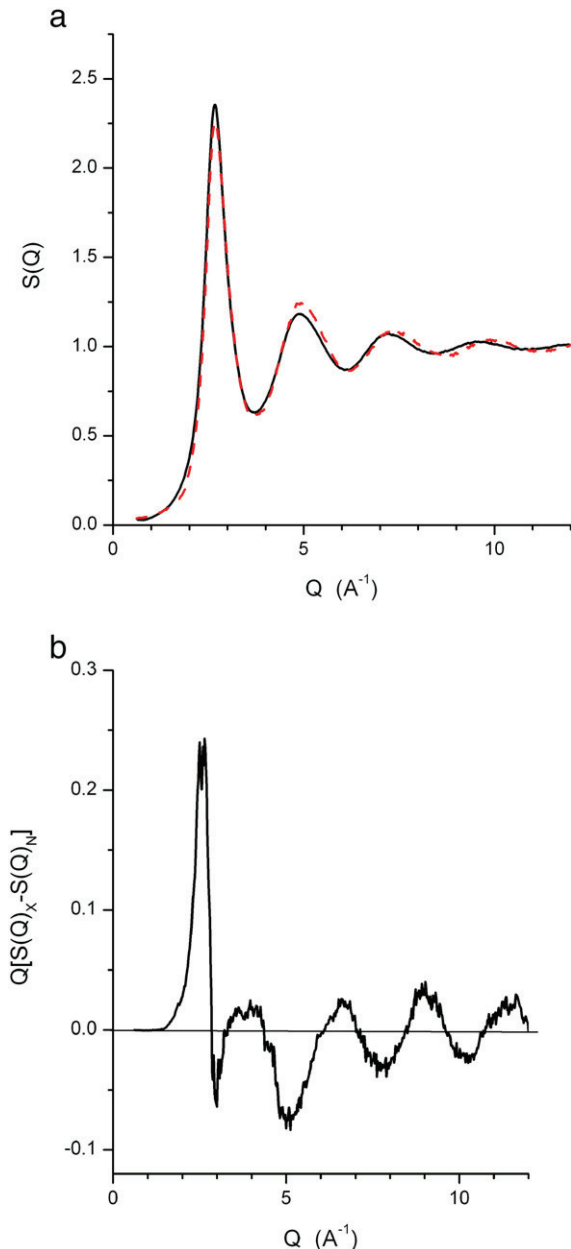


**Fig. 6.** (a) Static structure factors for liquid aluminum at 973 K determined by synchrotron X-ray diffraction  $S_X(Q)$  [93] (full black line) and neutron diffraction  $S_N(Q)$  (present work) (dashed red line) and (b) the quantity  $D(Q) = Q[S_X(Q) - S_N(Q)]$ .

the eutectic molten Al–Si alloy at both temperatures to be slightly smaller than 12. As 12 is the number of nearest neighbors in a face-centered cubic lattice and a molten metal hardly can be more close-packed than its solid counterpart this illustrates that the experimental determination of coordination number is questionable due to an overlap between the first and second coordination shells.

The temperature to which the Al–Si alloy was heated, 1373 K, is about 200 K lower than the  $T_b$  temperature as estimated from density measurements (see Fig. 1) but only slightly above the dissolution temperature  $T_d$ . According to density and viscosity measurements on other molten alloys [11,64,73], the microstructure inherited from the solid alloy is only partly dissolved at 1373 K. Fig. 5 shows that this is also the case for the structure on an atomic level. On further cooling, the dissolution keeps partly reversible and the eutectic Al–Si alloy during cooling from 1373 K recombines to be a two-phase system.

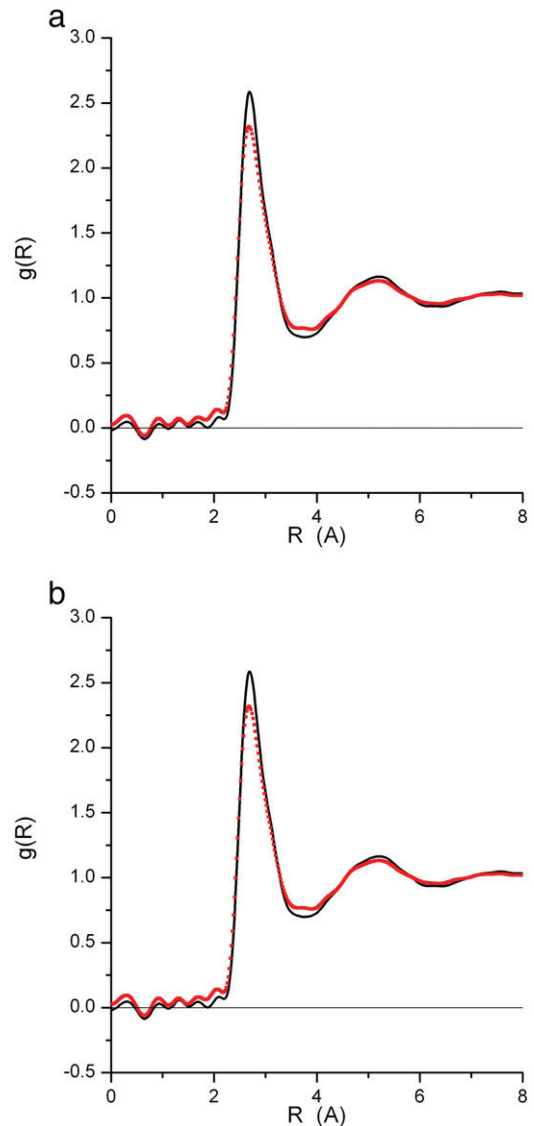


**Fig. 7.** Derived pair distribution functions  $g(R)$  for (a) molten Al and (b) molten  $\text{Al}_{87.8}\text{Si}_{12.2}$  at 973 K (full black lines) and 1373 K (dashed red lines).

One can expect that the observed structural difference would be larger and the irreversibility more pronounced if a larger superheat above the liquidus would have been possible to obtain, i.e. to reach a temperature larger than  $1560 \text{ K} \pm 30$ , the branching temperature.

## 6. Conclusions

The presented neutron diffraction measurements show that the molten eutectic Al–Si alloy after heating about 130 K above the liquidus contains particles of two kinds, one aluminum-rich and one silicon-rich. The silicon-rich particles are partly dissolved after a further heating of 400 K. This can be concluded from the fact that the main peak of  $S(Q)$  measured about 130 K above the liquidus is sharper after that the alloy has been heated to the higher temperature and then cooled to the same initial temperature. Strong support is thus given to earlier published data obtained by the  $\gamma$ -ray absorption technique on the density of the molten eutectic Al–Si that after melting the alloy is inhomogeneous up to a temperature well above the liquidus.

The difference in shape between the static structure factors measured by neutron diffraction and X-ray diffraction measurements

on molten aluminum has been clearly demonstrated. The difference which is due to ion–electron correlations is found to be more accentuated and to extend to considerably larger wavevectors than in earlier works found in literature. In the case of neutron diffraction, the correction for inelastic scattering is in this context of great importance.

Moreover, the presented results illustrate the difficulty to experimentally determine a static structure factor that can be used for detailed comparisons with theoretical predictions and with *ab initio* molecular dynamics simulations.

## Acknowledgements

Ames Laboratory is operated for the U.S. Department of Energy by Iowa State University under Contract No. W-7405-Eng-82. JRM's contribution was sponsored by the U. S. Department of Energy (DOE), Basic Energy Sciences, Materials Sciences and Engineering Division. The authors want to express their thanks to D.J. Sordelet who initiated the project and participated in the experiments. Furthermore, the authors are thankful to the Institute Laue-Langevin, Grenoble, France, for awarding beam time at the ILL reactor and to G. Cuello for his never failing willingness to assist during the measurements.

## References\*

- [1] W.E. Brower Jr., S.C. Megli, *Mater. Sci. Eng.*, A 133 (1991) 846–849.
- [2] V. Manov, A. Rubshtein, A. Voronel, P. Popel, A. Vereshagin, *Mater. Sci. Eng.*, A 179 (1994) 91–96.
- [3] M. Calvo-Dahlborg, *Mater. Sci. Eng.*, A 226–228 (1997) 833–845.
- [4] M. Calvo-Dahlborg, J.M. Ruppert, E.D. Tabachnikova, V.Z. Bengus, U. Dahlborg, F. Häussler, V.E. Sidorov, P.S. Popel, *J. Phys. I France* 11 (2001) 4–41–4–49.
- [5] V. Manov, P. Popel, E. Brook-Levinson, V. Molokanov, M. Calvo-Dahlborg, U. Dahlborg, V. Sidorov, L. Son, Yu. Tarakanov, *Mater. Sci. Eng.*, A 304–306 (2001) 54–60.
- [6] Q.G. Meng, J.K. Zhou, H.X. Zheng, J.G. Li, *Scr. Mater.* 54 (2006) 777–781.
- [7] H. Sheng, X. Zeng, Q. Hu, F. Deng, *J. Rare Earths* 28 (2010) 282–285.
- [8] M. Rajabi, A. Simchi, P. Davami, *Mater. Sci. Eng.*, A 492 (2008) 443–449.
- [9] U. Dahlborg, M. Calvo-Dahlborg, *Mater. Sci. Eng.*, A 283 (2000) 153–163.
- [10] P.S. Popel, M. Calvo-Dahlborg, U. Dahlborg, *J. Non-Cryst. Solids* 353 (2007) 3243–3253.
- [11] I.G. Brodova, P.S. Popel, G.I. Eskin, *Liquid metal processing: application to aluminium alloy production*, in: J.N. Fridlyander, D.G. Eskin (Eds.), *Advances in Metallic Alloys*, Taylor & Francis, London, 2002.
- [12] M.A. Taha, N.A. El-Mahallawy, R.M. Hamouda, *Mater. Des.* 23 (2002) 195–200.
- [13] Z. Chen, W. Jie, R. Zhang, *Mater. Lett.* 59 (2005) 2183–2185.
- [14] J. Barbosa, C. Silva Ribeiro, A. Caetano Monteiro, *Intermetallics* 15 (2007) 945–955.
- [15] X. Qi, J. Tang, S. Li, D. Zeng, *Trans. Nonferrous Met. Soc. China* 17 (2007) 887–892.
- [16] I.L. Ferreira, J.E. Spinelli, B. Nestler, A. Garcia, *Mater. Chem. Phys.* 111 (2008) 444–454.
- [17] J. Zhang, B. Li, M. Zou, C. Wang, L. Liu, H. Fu, *J. Alloys Compd.* 484 (2009) 753–756.
- [18] C. Wang, J. Zhang, L. Liu, H. Fu, *J. Alloys Compd.* 508 (2010) 440–445.
- [19] H. Sheng, X. Zeng, J. Zou, S. Xie, *J. Rare Earths* 28 (2010) 447–450.
- [20] A. Bendijk, R. Delhez, L. Katgerman, Th.H. De Keijser, E.J. Mittemeijer, N.M. Van Der Pers, *J. Mater. Sci.* 15 (1980) 2803–2810.
- [21] X.F. Li, F.Q. Zu, L.J. Liu, J. Yu, B. Zhou, *Phys. Chem. Liq.* 45 (2007) 531–539.
- [22] Y. Birol, *J. Alloys Compd.* 439 (2007) 81–86.
- [23] T. Hosch, R.E. Napolitano, *Mater. Sci. Eng.*, A 528 (2010) 226–232.
- [24] S.P. Nikanorov, M.P. Volkov, V.N. Gurin, Yu.A. Burenkov, L.I. Derkachenko, B.K. Kardashev, L.L. Regel, W.R. Wilcox, *Mater. Sci. Eng.*, A 390 (2005) 63–69.
- [25] H.K. Feng, S.R. Yu, Y.L. Li, L.Y. Gong, *J. Mater. Process. Technol.* 208 (2008) 330–335.
- [26] W.D. Griffiths, D.G. McCartney, *Mater. Sci. Eng.*, A 216 (1996) 47–60.
- [27] S. Nafisi, D. Emadi, M.T. Shehata, R. Ghomashchi, *Mater. Sci. Eng.*, A 432 (2006) 71–83.
- [28] D.M. Rosa, J.E. Spinelli, A. Garcia, *Mater. Lett.* 60 (2006) 1871–1874.
- [29] R. Venkataramani, R. Simpson, C. Ravindran, *Mater. Charact.* 35 (1995) 81–92.
- [30] J. Wang, S. He, B. Sun, Q. Guo, M. Nishio, *J. Mater. Process. Technol.* 141 (2003) 29–34.
- [31] M. Gupta, E.J. Laverna, *J. Mater. Process. Technol.* 54 (1995) 261–270.
- [32] M. Gupta, S. Ling, *J. Alloys Compd.* 287 (1999) 284–294.
- [33] H.S. Dai, X.F. Liu, *Mater. Charact.* 59 (2008) 1559–1563.
- [34] P. Li, V.I. Nikitin, E.G. Kandalova, K.V. Nikitin, *Mater. Sci. Eng.*, A 332 (2002) 371–374.
- [35] S. Hegde, K. Narayan Prabhu, *J. Mater. Sci.* 43 (2008) 3009–3027.
- [36] J. Wang, J. Qi, H. Du, Z. Zhang, *J. Iron. Steel Res. Int.* 14 (2007) 75–78.
- [37] R. Zhang, Q. Cao, S. Pang, Y. Wei, L. Liu, *Sci. Technol. Adv. Mater.* 2 (2001) 3–5.
- [38] N. Iqbal, N.H. van Dijk, V.W.J. Verhoeven, W. Montfroofij, T. Hansen, L. Katgerman, G.J. Kearley, *Acta Mater.* 51 (2003) 4497–4504.
- [39] S. Mudry, T. Lutsyshyn, *J. Alloys Compd.* 367 (2004) 289–292.
- [40] S. Takeda, S. Harada, S. Tamaki, Y. Waseda, *J. Phys. Soc. Jpn* 60 (1991) 2241–2247.
- [41] S. Takeda, Y. Kawakita, M. Inui, K. Maruyama, S. Tamaki, Y. Waseda, *J. Non-Cryst. Solids* 205–207 (1996) 365–369.
- [42] Y. Waseda, *The structure of non-crystalline materials, liquids and amorphous solids*, McGraw-Hill, New York, 1980.
- [43] K.E. Larsson, U. Dahlborg, D. Jovic, in: *Inelastic Scattering of Neutrons*, Proceedings of the IAEA Symposium, Vienna, vol. 1, 1965.
- [44] J.-P. Gabathuler, S. Steeb, P. Lamparter, *Z. Naturforsch., A: Phys. Sci.* 34 (1979) 1305–1313.
- [45] C.A. Becker, M.J. Kramer, *Modell. Simul. Mater. Sci. Eng.* 18 (074001) (2010) 1–15.
- [46] O.S. Roik, O.V. Samsonnikov, V.P. Kazimirov, V.E. Sokolskii, M. Galushko, *J. Mol. Liq.* 151 (2010) 42–49.
- [47] J.M. Stallard, C.M. Davis Jr., *Phys. Rev. A* 8 (1973) 368–376.
- [48] R. Wang, W. Lu, L.M. Hogan, *Mater. Sci. Eng.*, A 348 (2003) 289–298.
- [49] M.M. Haque, A.F. Ismail, *J. Mater. Process. Technol.* 162–163 (2005) 312–316.
- [50] X. Bian, W. Wang, J. Qin, *Mater. Charact.* 46 (2001) 25–29.
- [51] X. Song, X. Bian, J. Zhang, J. Zhang, *J. Alloys Compd.* 479 (2009) 670–673.
- [52] G. Heiberg, L. Arnberg, *J. Light. Met.* 1 (2001) 43–49.
- [53] C.L. Xu, Q.C. Jiang, *Mater. Sci. Eng.*, A 437 (2006) 451–455.
- [54] P. Srirangam, M.J. Kramer, S. Shankar, *Acta Mater.* 59 (2011) 503–513.
- [55] U. Dahlborg, M.J. Kramer, M. Besser, J.R. Morris, M. Calvo-Dahlborg, *Physica B* (submitted for publication).
- [56] D. Jovic, I. Padureanu, S. Rapeanu, *Liquid Metals* 1976, *Inst. Phys. Conf. Ser.* 30 (1977) 120–125.
- [57] S. Mudry, A. Korolyshyn, I. Shtablavyi, *J. Phys. Conf. Ser.* 98 (012016) (2008) 1–4.
- [58] I. Shtablavyi, S. Mudry, V. Mykhaylyuk, J. Rybicki, *J. Non-Cryst. Solids* 354 (2008) 4469–4474.
- [59] P.A. Egelstaff, N.H. March, N.C. McGill, *Can. J. Phys.* 52 (1974) 1651–1659.
- [60] P.S. Popel, E.L. Demina, E.L. Arkhangelskii, B.A. Baum, *Teplofizika Vysokikh Temperatur.* 25 (1987) 487–491.
- [61] W.M. Wang, X.F. Bian, H.R. Wang, Z. Wang, L. Zhang, Z.G. Liu, J.M. Liu, *J. Mater. Res.* 16 (2001) 3592–3598.
- [62] T. Magnusson, L. Arnberg, *Metall. Mater. Trans. A* 32 (2001) 2605–2613.
- [63] P.S. Popel, O.A. Chikova, V.M. Matveev, *High Temp. Mat. Process* 4 (1995) 219–233.
- [64] U. Dahlborg, M. Calvo-Dahlborg, P.S. Popel, V.E. Sidorov, *Eur. Phys. J. B* 14 (2000) 639–648.
- [65] M. Calvo-Dahlborg, P.S. Popel, M.J. Kramer, M. Besser, J.R. Morris, U. Dahlborg, *J. Alloys, Compd.* 550 (2013) 9–22.
- [66] V.F. Degtyareva, G.V. Chipenko, I.T. Belash, O.I. Barkalov, E.G. Ponyatovskii, *Phys. Status Solidi A* 89 (1985) K127–K131.
- [67] J.A. Knapp, D.M. Follstaedt, *Phys. Rev. Lett.* 58 (1987) 2454–2458.
- [68] P.S. Popel, V.E. Sidorov, *Mater. Sci. Eng.*, A 226–228 (1997) 237–244.
- [69] O.A. Korzhavina, I.G. Brodova, V.I. Nikitin, P.S. Popel, I.V. Polents, *Raspilvy* 1 (1991), p. 10, in: I.G. Brodova, P.S. Popel, G.I. Eskin (Eds.), *Liquid Metal Processing: Application to Aluminium Alloy Production*, in: J.N. Fridlyander, D.G. Eskin (Eds.), *Advances in Metallic Alloys*, Taylor & Francis, London, 2002.
- [70] G. Sivkov, D. Yagodin, S. Kofanov, O. Gornov, S. Volodin, V. Bykov, P. Popel, V. Sidorov, C. Bao, M. Calvo-Dahlborg, U. Dahlborg, D. Sordelet, *J. Non-Cryst. Solids* 353 (2007) 3274–3278.
- [71] V.E. Sidorov, M. Calvo-Dahlborg, U. Dahlborg, P.S. Popel, S. Chernoborodova, *J. Mater. Sci.* 35 (2000) 2255–2262.
- [72] V. Sidorov, O. Gornov, V. Bykov, L. Son, R. Ryltsev, S. Uporov, S. Shevchenko, V. Kononenko, K. Shunyaev, N. Ilynykh, G. Moiseev, T. Kulikova, D. Sordelet, *Mater. Sci. Eng.*, A 449–451 (2007) 586–589.
- [73] R. Brandt, G. Neuer, *Int. J. Thermophys.* 28 (2007) 1429–1446.
- [74] N.J. Grant, *Rapid Solidification Processing*, 1970, Claitor Publ. Div, Los Angeles, in: I.G. Brodova, P.S. Popel, G.I. Eskin (Eds.), *Liquid Metal Processing: Application to Aluminium Alloy Production*, in: J.N. Fridlyander, D.G. Eskin (Eds.), *Advances in Metallic Alloys*, Taylor & Francis, London, 2002.
- [75] S. Wang, C.Z. Wang, F. Chuang, J.R. Morris, K.M. Ho, *J. Chem. Phys.* 122 (034508) (2005) 1–6.
- [76] S. Wang, C.Z. Wang, C.X. Zheng, K.M. Ho, *J. Non-Cryst. Solids* 355 (2009) 340–347.
- [77] K.H. Khoo, T.-L. Chan, M. Kim, J.R. Chelikowsky, *Phys. Rev. B* 84 (214203) (2011) 1–6.
- [78] J.R. Morris, U. Dahlborg, M. Calvo-Dahlborg, *J. Non-Cryst. Solids* 353 (2007) 3444–3453.
- [79] U. Dahlborg, M. Besser, M. Calvo-Dahlborg, G. Cuello, C.D. Dewhurst, M.J. Kramer, J.R. Morris, D.J. Sordelet, *J. Non-Cryst. Solids* 353 (2007) 3005–3010.
- [80] <http://www.ill.eu>
- [81] J.R.D. Copley, P. Verkerk, A.A. van Well, H. Fredrikze, *Comput. Phys. Commun.* 40 (1986) 337–357.
- [82] J.L. Yarnell, M.J. Katz, R.J. Wenzel, S.H. Koenig, *Phys. Rev. A* 7 (1973) 2130–2144.
- [83] U. Dahlborg, B. Kunsch, *Phys. Chem. Liq.* 12 (1983) 237–254.
- [84] M.-C. Bellissent-Funel, L. Bosio, J. Teixeira, *J. Phys. Condens. Matter* 3 (1991) 4065–4074.
- [85] O.J. Eder, B. Kunsch, J.-B. Suck, M. Suda, *J. Phys. (Paris)* 41 (1980) C8, 226–229 229.
- [86] T. Scopigno, U. Balucani, G. Ruocco, F. Sette, *Phys. Rev. E* 63 (011210) (2000) 1–7.
- [87] J.R.D. Copley, S.W. Lovesey, *Rep. Prog. Phys.* 39 (1975) 461–563.
- [88] S.W. Lovesey, *Theory of Neutron Scattering from Condensed Matter*, Oxford University Press, 1984.
- [89] X. Bian, W. Wang, *Mater. Lett.* 44 (2000) 54–58.
- [90] K. Laaziri, S. Kycia, S. Roorda, M. Chicoine, J.L. Robertson, J. Wang, S.C. Moss, *Phys. Rev. B* 60 (1990) 13520–13533.
- [91] S. Ansell, S. Krishnan, J.J. Felten, D.L. Price, *J. Phys. Condens. Matter* 10 (1998) L73–L78.
- [92] P.J. Dobson, *J. Phys. C: Solid State Phys.* 11 (1978) L295–L298.
- [93] M.J. Kramer, unpublished results.

\* By mistake the temperatures quoted in [79] for the measurements on molten aluminum were 980 K and 1380 K.